Structure and molecular conformation of anhydrous and of aqueous sphingomyelin bilayers determined by infrared and Raman spectroscopy

ARTICLE *in* JOURNAL OF MOLECULAR STRUCTURE · AUGUST 1991

Impact Factor: 1.6 · DOI: 10.1016/0022-2860(91)85001-J

6 AUTHORS, INCLUDING:

Douglas Borchman
University of Louisville
118 PUBLICATIONS **2,950** CITATIONS
SEE PROFILE

Marta Yappert
University of Louisville
95 PUBLICATIONS **2,524** CITATIONS
SEE PROFILE

Journal of Molecular Structure, 248 (1991) 1–24
Elsevier Science Publishers B.V., Amsterdam

Structure and molecular conformation of anhydrous and of aqueous sphingomyelin bilayers determined by infrared and Raman spectroscopy

Om P. Lamba[a], Douglas Borchman[a,1], S.K. Sinha[b], Sundeep Lal[c], M. Cecilia Yappert[c] and Marjorie F. Lou[d]

[a]*Department of Ophthalmology and Visual Sciences, University of Louisville School of Medicine, Kentucky Lions Eye Research Institute, Louisville, KY 40292 (USA)*
[b]*Department of Biophysics, All India Institute of Medical Sciences, New Delhi-110 029 (India)*
[c]*Department of Chemistry, University of Louisville, Louisville, KY 40292 (USA)*
[d]*Alcon Laboratories, Inc., Fort Worth, TX 76134 (USA)*

(Received 13 September 1990; in final form 1 March 1991)

Abstract

Fourier transform-infrared spectra of anhydrous sphingomyelin and sphingomyelin bilayers in aqueous and deuterium phases have been investigated in detail. Raman spectra of the aqueous gel have also been measured. From these vibrational data, the structure and the molecular conformation of the head group, interface region and the hydrocarbon chains have been deduced in the solid and bilayer phases of the lipid. Vibrational assignments for the prominent fundamental modes associated with secondary structure of the lipid and molecular conformation of sphingosine and acyl chains, peptide unit and phospho-choline moiety are proposed. Vibrationally complex O–H and N–H stretching and deformation regions of the peptide unit and of bilayer water molecules have been probed using isotopic deuterium substitution. Infrared data suggest a strong intermolecular hydrogen bonding for the 3-hydroxyl groups of the sphingosine chains and an unusual intramolecular hydrogen bonding for the amide protons to carbonyl oxygens in the bilayer. These hydrogen-bonding schemes are likely to increase membrane stability through lateral contacts which may play an important role in membrane regulatory functions. Second derivative infrared spectroscopy has been used to explore the structurally sensitive spectral regions such as carbonyl, methylene deformation and phosphate regions of the lipid. This application revealed many weak bands associated with the specific regions of the membrane structure. Temperature-induced cooperative conformational transitions in sphingomyelin biomembrane have been examined in the aqueous phase. Data suggest a two state order–disorder phase transition at 35 °C with a transition enthalphy of 6.5 kcal mol^{-1}, agreeing closely with the enthalpies derived for structurally similar systems. The hydrocarbon chains are packed in a pseudo- or distorted hexagonal lattice in the solid and the gel phases. Data also indicate the existence of a hybrid domain in which lipid molecules coexist over a wide temperature range in the vicinity of the transition temperature, but revealed no evidence of interdigitation of hydrocarbon chains proposed earlier. Raman data also suggest that at least 30% of the hydrocarbon chain segments adopt a gauche conformation in the gel phase as well as in the anhydrous solid at room temperature. This indicates a considerable non-rigid environment for the sphingolipid hydrocarbon chains in the anhydrous and gel phases.

[1]Author to whom correspondence should be addressed.

0022-2860/91/$03.50

INTRODUCTION

Sphingomyelin is a major phospholipid component of several biological tissues such as brain and nerve cells, in erythrocytes and in four major classes of serum lipoproteins [1–4]. Sphingomyelin also constitutes a major phospholipid of the ocular lens tissue in humans and of several mammalian cells. Its accumulation in brain, liver and spleen arteries is known to cause severe neurological disorders with diverse clinical symptoms [5,6]. In the ocular lens sphingomyelin constitutes about 60% of the total phospholipid composition, and its role is less clearly understood [7]. However, in aging lens tissue and in senile cataractous lenses significantly higher levels of sphingomyelin have been observed [8–10].

Lipid/water dispersions are widely used as model systems in studies of structure–function relationships of biological membranes. Sphingomyelin, like many other phospholipids, forms bilayer structures when hydrated, and undergoes a structural phase transition near physiological temperatures. Studies on the properties and phase behaviour of sphingomyelin are quite limited, compared to other similar phospholipids [11,12]. The phase behaviour of sphingomyelin has been investigated using surface balance techniques [13,14], low resolution, low angle X-ray diffraction, differential scanning calorimetry and electron microscopy [15,16]. No detailed three-dimensional structure derived from X-ray crystallography is known for this sphingolipid, although some information regarding orientation of acyl and sphingosine chains with respect to the phospho-choline moiety is available [16]. In recent years, only three initial reports on Raman studies have appeared [17–19]. Mendelsohn et al. [17] have studied the melting behaviour of anhydrous sphingomyelin, whereas Fairman [18] probed the phase behaviour of aqueous bilayers in the optical skeletal region only. Fairman [18] has reported a two-state phase transition, while data on synthetic sphingomyelin composed of a single hydrocarbon chain (C24:0) indicate a three-state phase transition with presence of considerable interdigitation of hydrocarbon chains in the bilayer leaflet [19]. No structural details of the phase transition are available in the literature, especially by Fourier transform infrared spectroscopy.

Infrared and Raman spectroscopy have emerged as powerful non-destructive structural probes of biological membranes, providing a wealth of molecular information that no other single technique offers. In this paper, we present a detailed and comprehensive infrared study of the anhydrous and gel phases of bovine brain sphingomyelin. Raman spectra of the aqueous bilayers have also been obtained at ambient temperatures. Vibrational assignments for prominent fundamental modes specific to the sphingosine chain, phospho-choline moiety, peptide unit, acyl chains and the water molecules forming a hydration

belt around the polar region are proposed for the first time for this molecule. These fundamental modes, originating from concerted molecular motions in the bilayer, are understood in terms of molecular conformation and membrane structure. Deuterium substitution is used as a molecular probe to examine vibrationally complex O–H and N–H stretching regions, the amide I and II regions of the membrane interface, and also the librational modes of bilayer water. A detailed infrared study of the gel–crystalline phase transition of aqueous bilayers is also presented. Molecular events occurring during the phase transition are correlated with structural features of the bilayer.

MATERIALS AND METHODS

Preparation of membrane bilayers

High-purity samples of bovine brain sphingomyelin were commercially obtained from Sigma (St Louis, MO) and used without further purification. Purity and integrity of samples prior to use were checked by thin layer chromatography. Lipid was extracted in a chloroform–methanol mixture (2:1, v/v) as described previously [20]. Extracted lipid was dried in an oxygen-free inert atmosphere of argon. The dried lipid was then lyophilized further to remove remnant solvent traces. Liposomes were prepared by dispersing lyophilized lipid in an aqueous buffer consisting of 5 mM HEPES and 100 mM KCl at pH 7.4. Deuterated samples were prepared by dissolving anhydrous lipid in a D_2O buffer similar to that described for the aqueous buffer. Solid samples were prepared by dispersing anhydrous lipid in a KBr matrix.

Instrumentation

Infrared spectra were recorded on a Nicolet 7199C Fourier transform infrared spectrometer equipped with a TGS detector. Typically 100 interferograms were combined and apodized with a triangular function which gave effective resolution of 2.0 cm^{-1}. Temperature control was achieved using a Fenewal variable temperature unit from Wilmad Glass (New Jersey). Temperature was monitored to within $\pm 0.1\,^{\circ}C$ by a copper–constantan thermocouple. An average heating rate of $0.25\,^{\circ}C\ min^{-1}$ was maintained by increasing temperature in steps of $5\,^{\circ}C$ with a waiting period of 20 min.

Signal averaging, data smoothing using the Savitsky–Golay algorithm, polynomial baseline corrections, spectral subtractions, derivative-enhanced resolution and related spectral routines were performed on-line with PCIR software (version 2.1) obtained from Nicolet Analytic Division. Second derivative infrared data were smoothed to an extent which did not distort the line frequency, intensity or shape of the bands.

Samples for the Raman work were sealed in a pyrex glass capillary cell

(Kimax #34507), which was mounted in a sample illuminator. Raman spectra were excited with the 488.0 nm radiation of a Coherent Innova-70 argon ion laser, using about 100 mW of power at the sample. The scattered radiation was collected in right-angle configuration and was analyzed in a Jasco NR-1000 double monochromator equipped with a thermoelectrically chilled Hamamatsu photomultiplier-R464 tube and a digital photon counting system. Use of high resolution holographic gratings permitted the acquisition of spectra free of ghosts and other artifacts. Non-coherent emission lines were removed by using a narrow band interference filter placed at the laser head. Photon counts were read at intervals of 1 cm^{-1} with an integration time of 1 sec. Raman spectra illustrated below are the average of 3–4 scans and were recorded with a slit width of 6 cm^{-1}. Spectra were calibrated with standard inorganic sulphate and nitrate ions which resulted in peak accuracy better than ± 2 cm^{-1}.

Statistical evaluation of the lipid phase transition

The experimental data points were used to compute phase transition parameters. The data were fitted to the equation

$$\text{Frequency} = P_1 + P_2/[1 + (P_3/T)^{P_4}]$$

using a non-linear least-squares algorithm. P_1 is the minimum wavenumber in the phase transition curve, P_2 is the magnitude of the transition while P_3 and P_4 are the transition temperature and relative cooperativity, respectively. Further details of these parameters and enthalpy computations appear elsewhere [21].

RESULTS AND DISCUSSION

The molecular structure of sphingomyelin can be represented as shown in Fig. 1. The molecule has a constant-length, 18-carbon sphingosine chain and an amide-linked variable fatty acid chain. Natural sphingomyelin obtained from bovine brain comprises a variety of fatty acid chains ranging from C16 to C24. The saturated stearoyl chain, C18:0, and the unsaturated nervonoyl chain, C24:1, are the two dominant species, comprising approximately 2/3 of the total composition of acyl chains [18]. Other less abundant species of various carbon lengths are given in Fig. 1. Apparently more than 50% of the acyl chains comprising a hydrocarbon tail are longer than the constant sphingosine chain, reflecting an asymmetric chain length in the bilayer leaflets.

Spectral data and their assignments

Detailed vibrational assignments for sphingomyelin are not available in the literature. However, many of the prominent spectral features can be assigned

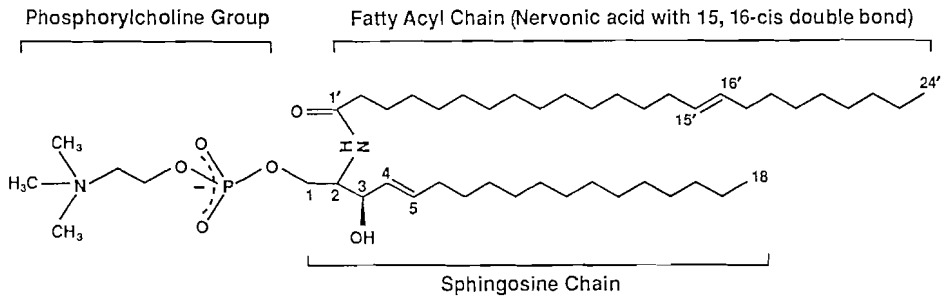

Fatty acid composition and their abundance:

Principal chains – 18:0 ; 34%
24:1 ; 33%

and, less abundant chains – 16 : 1, 18 : 1, 22 : 0, 24 : 0 } 33%

Fig. 1. Molecular structure of the bovine brain sphingomyelin. The structure depicts an unsaturated fatty acyl chain of nervonic acid with a 15,16-*cis* double bond. Composition of the fatty acid chains of varying carbon lengths, with their natural abundance, is given at the bottom of the figure.

from the comparative studies of the model lipid systems and the specific molecular components such as phospho-choline group, peptide unit, and sphingosine and acyl chains. The normal modes of a molecular unit in a similar force field usually occur in a relatively narrow frequency range with a well-defined intensity pattern in both infrared and Raman spectra. This has led to the identification and characterization of several fundamental modes in sphingomyelin. To verify these assignments, especially the N–H and O–H modes and the librational modes of bilayer water, the spectra of the solid and of the aqueous and deuterated gels were also examined.

A two-state phase transition observed at 35 °C in the sphingomyelin is discussed below (The Phase Transition). This section deals only with the vibrational assignments of the conformation-sensitive fundamental modes associated with the structural changes within specific regions of the membrane bilayer. In our discussion of the infrared and Raman band assignments, the gel phase refers to the data obtained at 25 °C, below the transition temperature. For the sake of simplicity in data presentation and interpretation, the results are given by spectral region. A complete summary of the vibrational assignments along with their molecular descriptions appears in Table 1.

The 3000–2800 cm^{-1} region

The 3000–2800 cm^{-1} spectral region in the infrared and Raman spectra of the phospholipids is very complex. In sphingomyelin this region is primarily

TABLE 1

Observed infrared and Raman active vibrational modes (cm^{-1}) and their assignments in sphingomyelin at 25°C

Infrared			Raman	
Aqueous bilayer	Solid in KBr	Deuterated gel	Aqueous bilayer	Assignments[a]
3419 sb		3420 sb		asym. stretch, H_2O
	3440 b, sh	3405 m, sp		O-H stretch, hydroxyl group
	3283 m, sp 3195 b, sh			N-H stretch, peptide unit
3258 b, sh			3235 sb	sym. stretch, H_2O
3080 w, sh	3080 w, sp			2× (Amide II)
			3045 vw	?
3006 w, sp	3007 w, sp	3006 w, sp		C-H stretch, -HC=CH- moiety
2956 w, sp	2957 m, sp	2956 w, sp	2957 vw	asym. stretch, CH_3 groups
			2932 w, b	2×1456
			2897 w, b	2×1440
2918 s, sp	2918 s, sp	2918 s, sp	2881 s, sp	asym. stretch, CH_2 groups
2872 w, sp	2872 w	2872 vw	2860 w, sh	sym. stretch, CH_3
2850 s, sp	2850 s, sp	2850 s, sp	2846 s, sp	sym. stretch, CH_2 groups
1645 s			1644 vvw	HOH deformation, H_2O
1658 sh	1658 sh	1658 sh	1672 w, b	-C=C- stretch, double bond moiety
1636 sh	1641 sp	1633 m, b	1660 m, b	Amide I
1553 m	1547 m, sp			Amide II
			1488 vw	
1493[b] sh	1493 vw	1493 w		
1479[b] vw	1479 w	1479 w		
1468 s, sp	1468 s, sp	1468 s, sp	1456 sh 1440 m, sp	C-H in-plane bend, CH_2 groups
1455[b] vw	1455 vw	1455 vw		
1437[b]	1437 vw			
1422[b] w	1422 w			
1342[c] w	1342 w	1342 w		
1378 w, sp	1378 w, sp	1378 w, sp	1370 w	C-H bend, CH_3 groups
1299[c] w	1313 vw	1313 vw		
			1298 vs	CH_2, twist
1276[c] vw	1276 w	1276 vw		
1245[c] sh	1245 s	1245 sh		
1228 mb 1214 mb	1231 mb 1211 sh	1231 vw 1211 mb		asym. stretch, PO_2^- group
1200[c] vw	1200 vw			
	1180 vw			
1085 s, db	1091 s, db	1085 s, db	1095 b	sym. stretch, PO_2^-
1057 m	1056 m	1056 w, sh	1072 sp	-C-O-P-O-C diester stretch
		1017 m, sp		N-D stretch, Amide II

TABLE 1 (continued)

Infrared			Raman	
Aqueous bilayer	Solid in KBr	Deuterated gel	Aqueous bilayer	Assignments[a]
970 m, sp	969 m, sp	970 sp	960 w	
923 w, sp	924 w	923 w		
			890 w	C–C stretch, acyl chain
873 w	875 w	873 w	873 w	deformation mode, choline group
839 w	836 w, db 817 w	839 w		
765 w	763 w	765 w	765 w	
720 m, sp	721 m, sp	720 sp	717 sp	CH_2, rock
700 mb				ip rock, H_2O
580 mb				opl wag, H_2O
		517 mb		ipl rock, D_2O
		≈ 410[d] mb		opl wag, D_2O

Abbreviations: w, weak; vw, very weak; b, broad; m, medium; mb, medium broad; s, strong; sp, sharp; sh, shoulder; db, doublet; ipl, in-plane libration; opl, out-of-plane libration.
[a]For notations used see text.
[b]Modes constitute CH_2 band progression.
[c]Modes constitute CH_2 band progression.
[d]Not revealed due to the cut-off limit of the spectrometer.

dominated by the contributions from the methylene and methyl symmetric and antisymmetric stretching fundamental modes. Infrared spectra of the anhydrous and of the aqueous and deuterated gels in the stretching region (3800–2700 cm^{-1}) are shown in Fig. 2, whereas the Raman spectrum of the corresponding aqueous gel for the same region appears in Fig. 3. As expected, hydrocarbon chain bands are predominant in all the spectra. This region is additionally complicated by three factors: (i) existence of several species of hydrocarbon chains of various lengths, each contributing its own vibrational mode and resulting in increased broadening of the bands, (ii) inter- and intramolecular interactions among methylene groups of adjacent bilayers, and (iii) involvement of Fermi resonance interaction between the symmetric C–H stretching fundamental mode of the methylene group at the zone centre and a continuum of second harmonics and binary combinations of methylene deformation modes extended over the entire Brillouin zone [22].

Infrared spectra of the aqueous sphingomyelin gel show four distinct peaks located at 2956, 2918, 2872 and 2850 cm^{-1} (see Fig. 2), whereas the Raman spectrum indicates a complex band profile of six partially resolved bands oc-

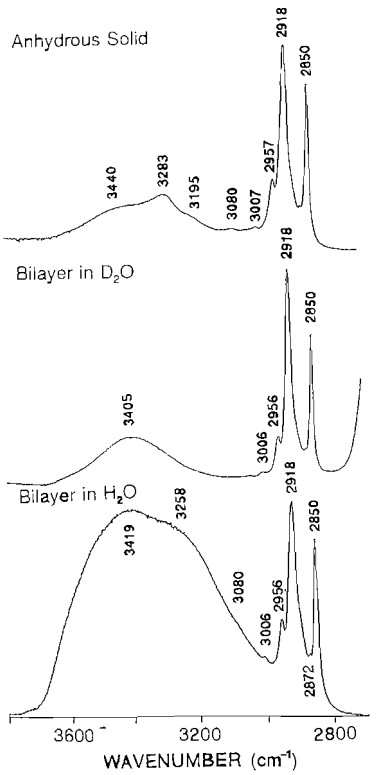

Fig. 2. Fourier transform infrared spectra of sphingomyelin in the C-H and O-H stretching regions, 2700-3800 cm^{-1}: bottom, aqueous bilayer gel phase prepared from aqueous buffer (5 mM HEPES and 100 mM KCl) at 25°C; middle, bilayers prepared from D_2O buffer at 25°C; top, anhydrous solid.

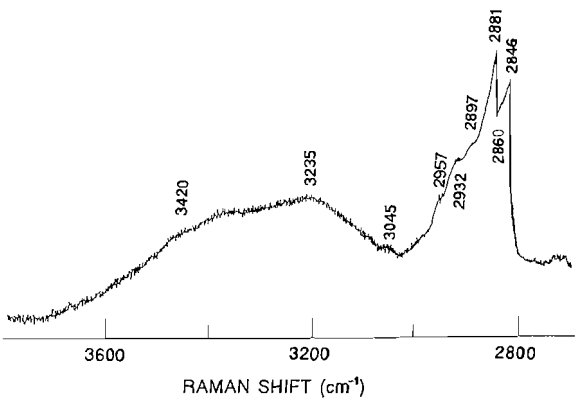

Fig. 3. Raman spectrum of aqueous sphingomyelin bilayer in the gel phase at 25°C in the C-H and O-H stretching regions, 2700-3800 cm^{-1}.

curring at 2957, 2932, 2897, 2881, 2860 and 2846 cm^{-1} (see Fig. 3). These modes are distinguished and are assigned below on the basis of their relative intensities observed in infrared and Raman spectra. The spectral features in the infrared spectrum arise from the antisymmetric and symmetric CH_2 stretching fundamental modes at 2918 and 2850 cm^{-1} (strong pair of infrared bands), while the antisymmetric and symmetric stretching modes of CH_3 groups are observed at 2956 and 2872 cm^{-1} (weak pair of infrared bands) [20,22,23]. The corresponding antisymmetric and symmetric Raman bands for the methylene groups are observed at 2881 and 2846 cm^{-1}, respectively (see Fig. 3). The weak bands at 2957 and 2860 cm^{-1} in the Raman spectrum occur near to the infrared bands, and therefore it is appropriate to assign them to antisymmetric and symmetric modes of methyl groups. Assignment of the 2932 cm^{-1} band to the symmetric terminal methyl group as proposed in ref. 19 appears to be dubious. This not only places the symmetric stretch higher than the antisymmetric one but is also inconsistent with the infrared assignments proposed for a large number of hydrocarbons [22,23].

The weak bands at 2897 and 2932 cm^{-1} observed in the Raman spectrum are probably the result of Fermi interaction involving the 2846 cm^{-1} stretching fundamental of the methylene group and the overtones of methylene deformation. It should be noted that methylene deformation modes are observed as a strong doublet at 1440 and 1456 cm^{-1} in the Raman spectrum and give overtone frequencies of 2880 and 2912 cm^{-1} with very low anharmonicities (Table 1). All these modes belong to the same symmetry species and therefore it is very likely that the modes at 2897 and 2932 cm^{-1} are the result of Fermi resonance rather than the result of inter- and intramolecular associations. Nevertheless, their origin has not been understood correctly. The Raman peak at 2897 cm^{-1} has been shown to be sensitive to intrachain conformational disorder and the lattice packing characteristics of acyl chains in lipids. The peak height intensity ratios I_{2846}/I_{2881} and I_{2932}/I_{2881} are used to characterize the lateral chain–chain, order–disorder rearrangements [24]. The peak height intensity ratios of 0.84 and 0.55, respectively, computed from the Raman data in the gel phase are slightly higher than the values of 0.78 and 0.36 reported for these bands in dipalmitoyl phosphatidylcholine (DPPC) gel at 25°C [24]. This indicates that roughly 34% of the rotamers are in a gauche conformation. This estimate is in agreement with the value of 29% determined from the infrared CH_2 symmetric stretching frequency using computations described previously [21]. Thus, we estimate that the sphingomyelin hydrocarbon chain region of the membrane is about 30% disordered.

The 3800–3000 cm^{-1} region

This is the second most complex region of the spectrum after the C–H stretching region. Absorption in this region is primarily dictated by the modes of water, hydroxyl groups of sphingosine chains and by N–H modes of the

peptide unit. Selective deuterium substitution allowed us to identify and characterize all of the modes in this region. As displayed in Fig. 2, the spectral region of the aqueous bilayers is dominated by two very intense absorption bands centered at 3419 and 3258 cm^{-1}. The consistency of the relative intensities of these bands in the infrared and Raman spectra (Fig. 3), and their appropriate frequency shift upon deuteration confirm that these bands must originate from the antisymmetric and symmetric stretching modes, respectively, of the coupled O–H oscillators of water molecules. The infrared spectrum of the anhydrous lipid reveals an interesting sharp band profile centred at 3283 cm^{-1} and two fairly isolated weak bands at 3007 and 3080 cm^{-1}, which otherwise remain obscured underneath intense water bands in the spectrum of aqueous bilayers. The 3283 cm^{-1} band profile is flanked by broad shoulders around 3440 and 3195 cm^{-1}. The bands at 3283, 3195 and 3080 cm^{-1} shifted by a factor of 1.36 upon deuteration, indicating that these bands must belong to N–H group vibrations. Indeed, all of these bands are characteristic of simple peptide units [25]. Since primary bonded N–H groups generate two broad bands near 3250 and 3180 cm^{-1}, the bands at 3283 and 3195 cm^{-1} are undoubtedly assigned to N–H stretching modes, while the origin of the 3080 cm^{-1} band is less clear [25]. However, the simultaneous disappearance of this band and the amide II band around 1548 cm^{-1} (see the next subsection and Fig. 4) clearly demonstrates that this band is, in fact, the first overtone of the amide II band.

The 3440 cm^{-1} shoulder in the spectrum of anhydrous sphingomyelin does not shift upon deuteration and appears as a single isolated peak at 3405 cm^{-1} in the spectrum of deuterated gel (Fig. 2). We assign this unequivocally to the hydrogen-bonded hydroxyl group at carbon 3 of the sphingosine chain. The hydroxyl group in all the natural sphingolipids usually assumes the D-configuration which orients away from the molecule. This steric arrangement favours strong polymeric hydrogen bonding which significantly enhances the capacity to establish lateral contacts with the surrounding lipid molecules. An unusually large band width of 150 cm^{-1} associated with the O–H mode in sphingomyelin confirms this assignment. Free or weakly bonded hydroxyl groups such as those observed in the L-configuration of synthetic sphingolipids are known to have very sharp band profiles with little or no hydrogen bonding [26]. A downward frequency shift of 35 cm^{-1} in the bilayer compared to the anhydrous lipid suggests that hydroxyl groups undergo further intermolecular hydrogen bonding, perhaps with the adjacent lipid layers or water molecules.

Finally, the weak band at 3006 cm^{-1} observed in the infrared spectra was found insensitive to isotopic substitution and is attributed to the C–H stretching modes arising from the *trans* –HC=CH– moiety at the 4 and 5 carbons of the sphingosine chain [19]. The *cis*-double bonds, constituting roughly about 50% of the hydrocarbon mixture in sphingomyelin, are expected to fall around the same frequency. Nevertheless, the trans and cis isomers are expected to differ in frequency by only a few wavenumbers and are unresolved in the spectra.

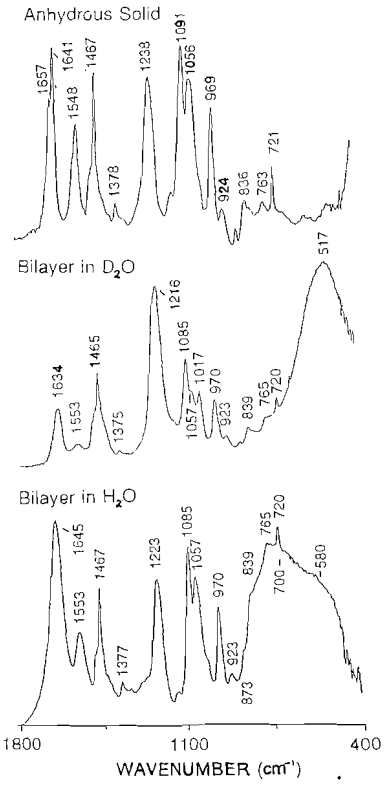

Fig. 4. Fourier transform-infrared spectra of sphingomyelin in the 1800–400 cm^{-1} region: bottom, aqueous bilayer gel phase prepared from aqueous buffer at 25 °C; middle, bilayers prepared from D_2O buffer at 25 °C; top, anhydrous solid.

The 1750–1500 cm^{-1} region

This region of the spectrum encompasses structurally and conformationally sensitive amide I and amide II bands from the peptide–sphingosine linkage and the modes from the –C=C– double bond moieties. Infrared spectra of the anhydrous lipid and of the aqueous and deuterated gels in the fingerprint region (1800–400 cm^{-1}) are shown in Fig. 4, while Fig. 5 depicts the Raman spectrum of the aqueous gel in the 1800–700 cm^{-1} region. The infrared spectrum of the anhydrous solid indicates a characteristic doublet at 1658 and 1641 cm^{-1} which is completely resolved in the second derivative spectrum as shown in Fig. 6. The doublet coalesces into a broad asymmetric band in the spectra of the gel phases, apparently due to inter- and intramolecular interactions with the solvent molecules. These broad bands centred around 1645 and 1634 cm^{-1}, respectively, in the spectra of the aqueous and deuterated gels (Fig. 4) are partially resolved in their second derivative spectra (Fig. 6). The band in the aqueous gel appears much wider (about 1.7 times the halfwidth of the band in

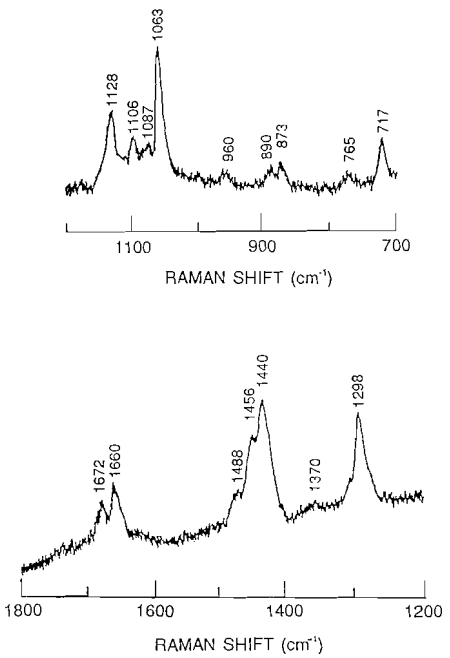

Fig. 5. Raman spectrum of aqueous sphingomyelin bilayer in the gel phase at 25°C in the 1800–700 cm^{-1} region.

the deuterated gel), primarily due to the serious overlapping from the HOH deformation mode of the water molecules expected around 1645 cm^{-1}. The lower component of the anhydrous doublet at 1641 cm^{-1} shifts to around 1633 cm^{-1} in the gel phases; the higher component is still discernible as a shoulder around 1658 cm^{-1} in the gel spectra (Fig. 6). In the Raman spectrum of the aqueous gel this doublet appears at the relatively higher frequencies of 1672 and 1660 cm^{-1} (Fig. 5). Levin et al. [19] have assigned the structural feature around 1672 cm^{-1} to the –C=C– stretch of the 4,5-*trans* double bond of the sphingosine chain and an extremely weak band around 1644 cm^{-1} to amide I in aqueous synthetic sphingomyelin. Structurally similar systems, cerebrosides and ceramides [27], also generate a peak around 1672 cm^{-1} which conclusively supports the above assignment. We, however, disagree with their assignment of the amide I peak. In the light of our deuteration study, studies of the solid and aqueous phases and the enhanced resolution of derivative peaks, we offer below a revised interpretation of the peaks in this region.

The amide I peak predominantly involves C=O stretch and is appreciably coupled to C–N stretch and N–H deformation modes, and therefore a relatively small shift upon deuteration is expected. The double bond, –C=C– moieties from sphingosine and acyl chains (Fig. 1), buried deeply in the hydrophobic core of the bilayers, involve no exchangeable protonic motions, and the cor-

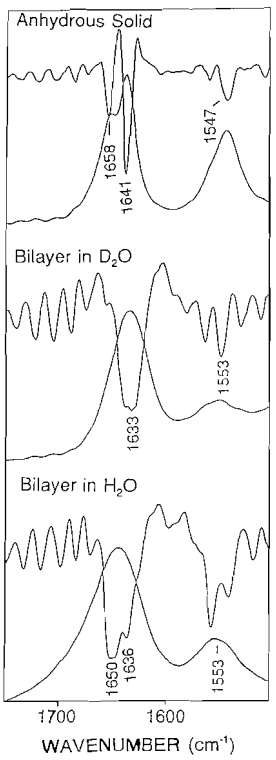

Fig. 6. Second-derivative Fourier transform-infrared spectra of sphingomyelin in the 1750–1500 cm^{-1} region: bottom, aqueous bilayer gel phase at 25°C; middle, bilayers in D_2O at 25°C; top, anhydrous solid. Data were smoothed prior to taking the derivative (order of smoothing 13×3).

responding vibrational band should remain unshifted upon deuteration. This is indeed observed in the deuterated spectrum (Fig. 6). The higher frequency component around 1658 cm^{-1} remains insensitive to deuteration, whereas the lower component shifts significantly downward. It is, therefore, appropriate to assign the higher component to the 4,5-*trans* double bond stretch of the sphingosine chain and the lower component primarily to amide I in the Raman as well as in the infrared spectra. Nevertheless, the lower component may involve contributions from the *cis* double bond, –C=C– moieties of the acyl chains present in natural sphingomyelin. The weak feature around 1644 cm^{-1} observed in the Raman spectrum by Levin et al. [19], is probably due to the HOH deformation mode of the water molecules involved in the bilayer H-bonding network for the following reasons. The intensity of this band is too weak for an amide I band, especially when all the fundamentals associated with the peptide unit are observed with appreciable intensity in the Raman as well as in the infrared spectra. Secondly, the stretching modes of water in the Raman spectrum appeared very close to the frequencies of water observed in the infrared

spectrum; therefore a weak bending mode of water close to 1645 cm^{-1} is expected in the Raman spectrum as well (see Fig. 5).

The 1547 cm^{-1} band observed in the infrared spectrum of anhydrous lipid is assigned to amide II (predominantly N–H bend and a little C–N stretch). This is confirmed by a deuteration shift of this band to 1017 cm^{-1} (Fig. 4). The observed isotopic shift of 1.52 is relatively higher than the actual value of 1.40 expected for a pure harmonic vibration. This band is reported at 1535 cm^{-1} in the Raman spectrum of the synthetic sphingomyelin gel [19]. Surprisingly, this band is not observed in our Raman spectrum of the gel phase (Fig. 5) or in the Raman spectrum of the natural anhydrous sphingomyelin obtained by Mendelsohn et al. [17]. Although, the total absence of the amide II band in the Raman spectrum is known [28], the difference between the spectra obtained by us and those reported by Levin et al. [19] is difficult to explain. One apparent difference noticed is that the natural bovine brain sphingomyelin is a mixture of six hydrocarbon chains whereas the synthetic sphingomyelin samples used in ref. 19 contain a single acyl chain, the lignoceroyl group. There are several other significant differences observed in terms of the nature of phase transition which are discussed below. The amide II band also shifts towards higher frequency in going from solid to solution, a shift quite opposite to that expected for an amide II band. The amide II band is known to shift towards a lower frequency in going from solid to solution due to breaking of hydrogen bonds [25]. A large anharmonicity associated with this band and the opposite shift in frequency are indicative of an unusual hydrogen-bonding scheme for the amide protons in the bilayer dispersion. Similar shifts for the amide I peak are also observed in the Raman spectra of anhydrous and gel ceramides and cerebrosides [27]. Crystallographic data [26] indicate that the peptide unit in this class of compounds assumes a planar, trans configuration, and orients perpendicularly to the parallel running axes of the sphingosine and acyl chains. This configuration strongly favours the increased interaction of the amide proton with the carbonyl oxygen. We propose an additional intramolecular hydrogen bonding of the amide proton to the carbonyl oxygen of the lipid.

The 1500–1350 cm^{-1} region

The infrared spectra of the anhydrous and of the gel phases of sphingomyelin are characterized by a sharp methylene deformation band at 1468 cm^{-1} which is by far the strongest band in this region, shown in Fig. 7. Also evident in the spectra is a progression of regularly spaced weak bands between 1405 and 1480 cm^{-1} and a weak band at 1378 cm^{-1} due to methyl deformation. The characteristic features of the progression are discussed below (methylene band progressions). The methylene deformation band is observed as a strong doublet at 1440 and 1456 cm^{-1} in the Raman spectrum of the aqueous gel (Fig. 5). Multiple components associated with the deformation mode in the Raman

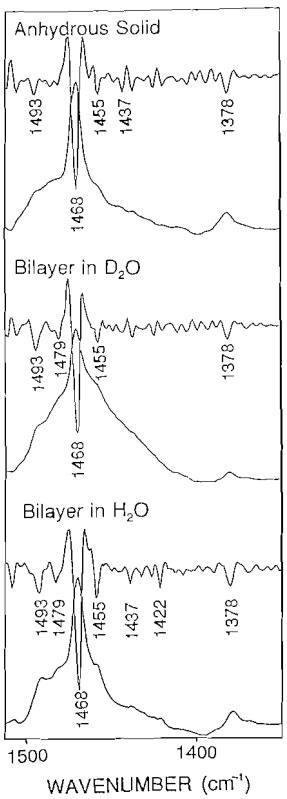

Fig. 7. Second-derivative Fourier transform-infrared spectra of sphingomyelin in the 1500–1350 cm^{-1} region: bottom, aqueous bilayer gel phase at 25°C; middle, bilayers in D_2O at 25°C; top, anhydrous solid. Data were smoothed prior to taking the derivative (order of smoothing 11×3).

spectra are sensitive to the type of packing of the hydrocarbon chains in the unit cell [29]. Of the commonly known hydrocarbon packings, only orthorhombic or monoclinic crystal lattices are known to exhibit substantial splittings, while triclinic and hexagonal lattices do not show any splittings [30,31]. We observed no splitting of this band in the Raman spectrum recorded at a relatively higher resolution. A similar conclusion is reached from the Raman data on synthetic sphingomyelin reported by Levin et al. [19]. Thus, these data demonstrate that acyl chains are packed in a pseudo- or distorted hexagonal lattice cell in the solid as well as in the gel phase. Preliminary X-ray data [16] available on sphingomyelin do not shed any light on the crystal packing of acyl chains or their relative orientations in the unit cell, and therefore an exact description of the bilayer structure should await more detailed high resolution X-ray diffraction data.

The 1350–1000 cm^{-1} region

Bands associated with the antisymmetric and symmetric PO_2^- stretches,

diester phosphate stretch, –C–O–P–O–C– stretch and C–C stretch optical skeletal modes of hydrocarbon chains are expected to fall in this region. Spectral profiles of the infrared (Fig. 4) and the Raman (Fig. 5) spectra are remarkably different in this region. As the phosphate vibrations in the lipids are well characterized in the infrared, the optical skeletal C–C stretching acyl chain modes are quantitatively understood from Raman. We discuss these modes separately.

The infrared spectrum shows a broad band at 1223 cm^{-1} and a sharp doublet at 1085 and 1057 cm^{-1} in the aqueous gel (Fig. 4). This band profile is strikingly similar to the spectra of a large number of model phospholipids and certain inorganic phosphates [32,33]. The bands at 1223 and 1085 cm^{-1} are identified as antisymmetric and symmetric stretches of the dioxyphosphate groups, respectively, while the characteristic band at 1057 cm^{-1} is assigned to the symmetric stretch of the diesterified phosphate, –C–O–P–O–C–, skeleton. These backbone vibrations, which determine the conformation of the entire head group, reveal many interesting features. The diesterified phosphate band behaves in a remarkably different manner to the dioxyphosphate vibrations upon dehydration and deuteration. While the dioxyphosphate bands shift drastically to higher frequencies upon dehydration, the diester stretch remains practically unchanged (Fig. 4). Upon deuteration the dioxyphosphate bands remain practically unshifted, while the diester phosphate stretch almost disappears or diminishes significantly in intensity. Note that the asymmetric stretch is completely overlapped by the strong bending mode of D_2O around 1210 cm^{-1} in the spectrum of the deuterated gel (Fig. 4).

The frequency shift upon dehydration could be explained by increased restriction of the phospho-choline moiety in the solid, as similar dehydration-induced changes have been observed in the infrared spectra of fully hydrated DPPC, a phospholipid with the identical polar head group [32,34]. Recent ^{31}P-NMR data have indicated a greater head group restriction in sphingomyelin, presumably due to the presence of an intramolecular hydrogen bond between the phosphate and either the amide or hydroxyl group [35,36]. These results strongly corroborate our findings concerning the intramolecular hydrogen-bonding scheme proposed for the amide protons (see above). The diester bond, –C–O–P–O–C–, which provides a conformational link between sphingosine chain and choline moiety, involves no exchangeable protons and one does not expect a frequency shift or a considerable loss of intensity upon deuteration. The observed intensity loss in the spectrum of the deuterated gel could be explained either by an underlying band which involves considerable coupling with the exchangeable protons of the water molecules or by a complex coupling with the nearby protons of the hydroxyl groups or amide proton, possibly through a hydrogen-bonding network. Similar loss of intensity in the diester band was observed in DPPC bilayers bound to cholate [37]. Nevertheless, these data clearly demonstrate the structural rearrangements occurring in the head groups within the bilayer phase.

The second derivative spectrum of the broad asymmetric stretch of the dioxyphosphate reveals two components in the spectra of anhydrous lipid and

of the gel phases as shown in Fig. 8. These components may reflect the presence of environmentally different phospho-choline heads. We, however, did not observe any splitting or structure in the symmetric dioxyphosphate or diester stretches. A well-defined band progression between 1340 and 1170 cm^{-1} is also evident and it is discussed below (methylene band progressions).

As mentioned above, information regarding trans–gauche isomerism can be obtained from the Raman spectra of the optical skeletal modes. These modes occur over a wide frequency range. However, in-phase and out-of-phase C–C stretching modes of the rigid hydrocarbon chain fall in a narrow frequency range, 1000–1050 cm^{-1}. The Raman spectrum displays a cluster of four bands at 1063, 1087, 1106 and 1128 cm^{-1} and a fairly isolated strong band at 1298 cm^{-1} (Fig. 5). The sharp bands at 1063 and 1128 cm^{-1} are the B_{1g} and A_g modes of all-trans chain segments [38] while the band at 1087 cm^{-1} results from structures containing gauche conformers. A small gauche population is evident from the intensity ratio, I_{1063}/I_{1087}, indicating disordering of the acyl chains. These results are in good agreement with our estimate of the percent-

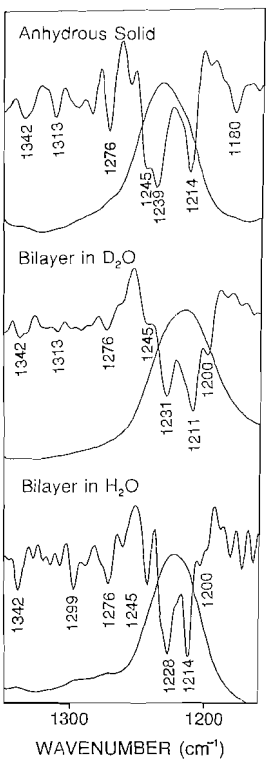

Fig. 8. Second-derivative Fourier transform-infrared spectra of sphingomyelin in the 1350–1100 cm^{-1} region: bottom, aqueous bilayer gel phase at 25°C; middle, bilayers in D_2O at 25°C; top, anhydrous solid. Data were smoothed prior to taking the derivative (order of smoothing 9×3).

age of the gauche rotamers discussed above and the previous Raman and X-ray studies [16,18]. Finally, the 1298 cm^{-1} mode, which is also one of the strongest bands in the Raman spectrum (Fig. 5), is the in-plane methylene twist [39]. It is interesting to note that most of the prominent fundamental modes of the hydrocarbon chains are either Raman active or displaced significantly from their infrared counterparts. Despite considerable disorder due to the presence of gauche isomers, the trans segments of the hydrocarbon chains appear to have maintained largely C_{2h} local symmetry. This appears to be consistent as all the known hydrocarbon chains depicted in Fig. 1 contain an even number of carbon atoms which usually favours higher chain symmetry.

The 1000–400 cm^{-1} region

This region of the infrared spectrum contains a large number of weak bands embedded in an ill-defined broad plateau with band maxima centered near 700 and 580 cm^{-1} in the spectrum of the aqueous gel (Fig. 4). Except for these broad bands, all the observed weak bands at 970, 923, 873, 839, 765 and 720 cm^{-1} are totally insensitive to deuterium substitution, indicating that these modes must originate either from the rigid head group, the phospho-choline moiety or from segments of the rigid C–C skeleton of acyl chains. The correct origin of these modes is difficult to understand, especially when a large number of acyl chains of varying length are present in sphingomyelin. We, therefore, did not attempt to characterize these modes in detail. However, there are many conflicting arguments regarding the origin and interpretation of several characteristic modes in this region which deserve attention. Some of the modes such as 717, 765, 873, 890 and 960 cm^{-1} (970 in infrared) are active both in the Raman and infrared, and could be seen in both spectra at about the same frequency. One group of workers has assigned the band around 717 cm^{-1} to C–N symmetric stretch of the C_4N^+ backbone of the choline group in the Raman [34,40–42], while another group has assigned a band around 720 cm^{-1} to the CH_2 rock in the infrared spectra [29,33]. The frequency and halfwidth of this band has been shown to be sensitive to hydration and cations [34,42]. The frequency and halfwidth of this band in our samples are very close to those observed in the gel phase of the fully hydrated DPPC [42]. The characteristic Raman-active doublet bands around 873 and 890 cm^{-1} have been identified as choline deformation and C_1–C_2 stretch with little contribution from methyl terminal C–C stretch, as noted in DPPC and dipalmitoyl phosphatidylethanolamine (DPPE) [43,44]. The intensity ratio, I_{873}/I_{890}, of these bands has been shown to be sensitive to the geometry of the interface region and lateral interactions with the choline head. The computed intensity ratio in sphingomyelin is similar to that observed in the DPPC bilayer, containing a lipid with the identical choline head group. This ratio is slightly lower than the ratios, 0.51 and 0.44, observed in DPPE [44] and sphingosine [27], respectively, which have no choline head groups. This supports the argument that a choline head

group does influence the interface geometry and contributes to the intensity of the 873 cm^{-1} band [43,44].

The broad envelope and its unresolved maxima at 700 and 580 cm^{-1} observed in the infrared spectrum of the aqueous gel are in fact very interesting features of this region. These low-lying librational modes of water molecules have never been interpreted in the spectra of hydrated lipids, especially when all biological functions of the membrane occur in aqueous medium. As these bands are associated with displacement of whole water molecules librating in a relatively weak intramolecular force field in the membrane matrix, their biological relevance cannot be ignored. In a free ion approximation, a water molecule generates two infrared-active librational modes, namely an in-plane rocking mode and an out-of-plane wagging mode [45,46]. A third libration, a twisting mode, appears very weakly in the infrared only because of the loss of C_{2v} symmetry for the water molecules. The fact that these bands shift approximately by a factor of $1/(2)^{1/2}$ upon deuteration and completely disappear on dehydration confirms that these bands essentially originate from the concerted librational motions of water molecules forming a bilayer organization. We have earlier characterized and identified these water librations in a varying asymmetric force field in crystal hydrates using several well-known criteria [45,46]. The 700 cm^{-1} band shifts to 517 cm^{-1} in the spectrum of the deuterated gel (Fig. 4). From our previous studies the 580 cm^{-1} band would be expected to shift to around 410 cm^{-1} upon deuteration. This band did not show up as it happens to fall right on the cut-off limit of the rock salt optics employed in our spectrometer. Based on the criteria discussed in refs. 45 and 46, we place the rocking motion at higher frequency than the wag. The water molecules, though distorted, appear to have maintained largely C_{2v} local symmetry in the membrane bilayer leaflet.

Methylene band progressions

As noted above infrared spectra exhibit two dominant progressions in the spectral interval 1492–1422 cm^{-1} and 1350–1200 cm^{-1}. The higher frequency progression consists of six weak bands, regularly spaced, at 1493 (head band), 1479, 1455, 1437, 1422 and 1405 cm^{-1} (Fig. 7), whereas five bands occurring at 1200 (head band), 1245, 1276, 1299 and 1342 cm^{-1} (Fig. 8) are identified in the lower frequency progression. The intensities of these progressions fall off rapidly as we move away from the head bands, and the positions of band maxima become less and less clear. Both progressions disappear on melting of the hydrocarbon chains above the transition temperature, suggesting that they are characteristic of the ordered trans segments of the acyl chain structure. These progressions are very similar to those observed in DPPC [29]. Band progressions for a finite chain length, the wagging or twisting modes of n coupled methylene groups, are identified from the expression given below. The phase differences, ϕ, allowed between adjacent groups are given by

$$\phi = k\pi/(n+1)$$

where $k=1, 2, 3 \ldots n$, is the number of nodes or antinodes in a standing wave pattern [39]. The splitting patterns and regular spacings observed between the frequency components of the two progressions are remarkably different. The splitting magnitude of the higher progression is roughly three times that observed in the lower one. The frequency patterns are characteristic of the specific length of the segment of chain, and the splitting magnitudes observed in sphingomyelin correspond to the chain lengths containing 15–30 carbon atoms. We believe that both progressions are the wagging–twisting progressions in sphingomyelin resulting from partial orientation of the trans segments of hydrocarbon chains.

The phase transition

Anhydrous sphingomyelin displays several polymorphic phase transitions, which, as in many other phospholipids, are hydration dependent [15]. Interestingly, in all of these phases hydrocarbon chains pack in a hexagonal-type structure. Increasing the amount of water to about 10%, causes the transition temperature to drop to 40 °C, after which it remains independent of hydration. Below the transition temperature, sphingomyelin exists in a bilayer structure with maximum hydration uptake of 42% [12]. This phase also assumes a β-type structure in which hydrocarbon chains are packed in a pseudo-hexagonal lattice with rotational disorder.

The temperature dependence of the infrared spectra of C–H stretching bands of the methylene groups of acyl chains is shown in Fig. 9. As can be seen, the stretching fundamental modes of methylene groups are extremely sensitive to the local environmental changes induced by temperature. With decreasing temperature an increase is observed in peak height and integrated intensity, and a decrease in bandwidth and a shift of frequency to lower wavenumbers. We have plotted the temperature-induced frequency changes for the stretching fundamentals in Fig. 10. Data in Fig. 10 for the heating and cooling cycles indicate no sign of hysteresis in the phase transition within the limits of experimental accuracy. This suggests that the bilayer phase is largely a non-heterogeneous structure. Results in Fig. 10 indicate a cooperative phase transition around 35 °C with a wide transition width relative to that for the glycerophospholipids. This suggests that the lipid molecules coexist in an intermediate phase over a wide temperature range, but reveals no additional transition between 0 and 60 °C.

Infrared as well as Raman data do not demonstrate any kind of splittings in going from the liquid-crystalline to gel phase, indicating that the bilayer structure-like liquid-crystalline phase largely packs in a pseudo-hexagonal lattice. Heating of the bilayer phase to 90 °C surprisingly did not yield substantial changes except general broadening of the conformation-sensitive bands of the phospho-choline moiety, the hydroxyl group and the amide I and II bands in

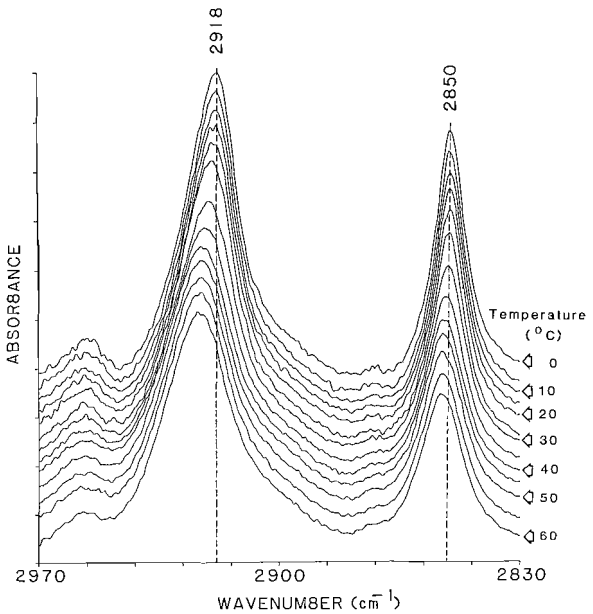

Fig. 9. Temperature-dependence Fourier transform-infrared spectra of the symmetric and antisymmetric stretching modes of methylene groups of hydrocarbon chains of aqueous sphingomyelin in the 2800–3000 cm^{-1} region. Spectra are obtained at temperature intervals of 5 °C listed to the right of each spectral trace. Each spectrum is baseline-corrected for the rising background of the O–H stretching modes of water.

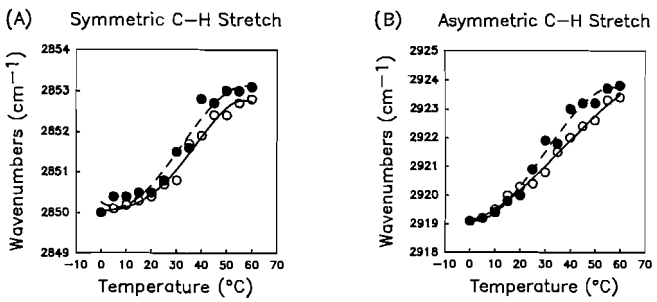

Fig. 10. Plot of the measured frequencies of the symmetric and antisymmetric vibrational modes of methylene groups vs. the temperature of the phase change for aqueous sphingomyelin; open circles, cooling cycle; solid circles, heating cycle.

the interface region, and the methyl and methylene groups (spectra not shown). This indicates an increased mobility for the hydrocarbon chains and relatively more freedom for the polar head group in the lipid. In synthetic sphingomyelin Levin et al. [19] has reported two transition temperatures at 48.5 and 54.5 °C, attributed to the interdigitation resulting from asymmetric packing of the lignoceroyl acyl chains in the leaflets of adjacent bilayers. It is surprising that the

natural sphingomyelin which contains a large number of hydrocarbon species of various asymmetric chain lengths did not show any evidence of interdigitation.

Differential calorimetric data on maximally hydrated bovine brain sphingomyelin [15] indicate two transitions in a narrow temperature range (30–38°C), whereas heat capacity curves on synthetic hydrated sphingomyelin [47] indicate one sharp transition between 30 and 50°C. The differences in the state of transition observed by different authors is perhaps due to the different composition of hydrocarbon chain species which exist in natural and synthetic sphingomyelin molecules and perhaps due to different hydration levels [48]. It is interesting to note that despite different acyl chain compositions, the computed enthalpy of 6.5 kcal mol^{-1} agrees closely with values obtained from calorimetric and heat capacity data [15,47] and the enthalpies computed for phrenosin and natural cerebrosides [27], suggesting that the lattice arrangements do not substantially differ in samples obtained from different sources.

CONCLUSIONS

A comprehensive vibrational analysis for almost all of the prominent infrared and Raman active fundamental modes has been discussed for the anhydrous and aqueous sphingomyelin molecules for the first time. Isotopic deuterium substitution of the anhydrous sphingomyelin led to the correct assignments of several fundamental modes, especially in the vibrationally complex O–H and N–H stretching and amide I and II regions. The data indicate an unusual intermolecular hydrogen-bonding scheme for the hydroxyl groups and intramolecular hydrogen bonding of the amide proton to the carbonyl oxygen which may provide an increased stability to the membrane bilayer. These different types of hydrogen-bonding schemes are likely to increase the lateral lipid contacts which may play a key role in regulating biological membrane functions. Both the infrared and Raman data reveal the presence of a significant population (30%) of gauche conformers in the gel phase, indicating disordering of the hydrocarbon chains. These chains are largely packed in a pseudo-hexagonal lattice confirming earlier findings.

ACKNOWLEDGEMENTS

We thank Mr. Raman Malhotra for providing technical assistance in recording Raman spectra. This work is supported by USPHS research grant EY-07975, the Kentucky Lions Eye Foundation, an unrestricted grant from Research to Prevent Blindness, Inc., and a gift from Alcon Laboratories, Fort Worth, Texas.

REFERENCES

1 G. Rouser, G.J. Nelson, S. Fleischer and G. Simon, in D. Chapman (Ed.), Biological Membranes, Vol. 1, Academic Press, London, 1968, p. 5.
2 R.M. Burton, in G. Schettler (Ed.), Lipid and Lipodoses, Springer-Verlag, Berlin, 1967, p. 122.
3 V.P. Skipskii, in G.J. Nelson (Ed.), Blood Lipids and Lipoproteins, Quantitative Composition and Metabolism, Wiley-Interscience, Toronto, 1972, p. 471.
4 K.P. Strickland, in G.B. Ansell, J.N. Howthrone and R.M.C. Dawson (Eds.), Forms and Functions of Phospholipids, Elsevier, Amsterdam, 1973, p. 9.
5 H.J. Fallon, J. Barwick, R.G. Lamb and H. Van den Bosch, J. Lipid Res., 16 (1975) 107.
6 I. Caras and B. Shapiro, Biochim. Biophys. Acta, 106 (1975) 63.
7 A. Spector, Invest. Ophthalmol. Vis. Sci., 25 (1984) 130.
8 R.M. Broekhuyse, Biochim. Biophys. Acta, 187 (1969) 354.
9 E. Cotlier, Y. Obara and B. Toftness, Biochim. Biophys. Acta, 530 (1978) 267.
10 G.L. Feldman, L.S. Feldman and G. Rouser, Lipids, 1 (1966) 161.
11 D. Chapman and D.F. Wallach, in D. Chapman (Ed.), Biological Membranes, Vol. 1, Academic Press, London, 1968, p. 125.
12 G.G. Shipley, in D. Chapman (Ed.), Biological Membranes, Vol. 2, Academic Press, London, 1973, p. 1.
13 D.O. Shah and J.H. Shulman, Lipids, 2 (1967) 21.
14 D.O. Shah and J.H. Shulman, Biochim. Biophys. Acta, 135 (1967) 184.
15 G.G. Shipley, L.S. Avecilla and D.M. Small, J. Lipid Res., 15 (1974) 124.
16 R.S. Khare and C.R. Worthington, Biochim. Biophys. Acta, 514 (1978) 239.
17 R. Mendelsohn, S. Sunder and H. Bernstein, Biochim. Biophys. Acta, 413 (1975) 329.
18 R. Fairman, Chem. Phys. Lipids, 23 (1979) 77.
19 I.W. Levin, T.E. Thompson, Y. Barenholz and C. Huang, Biochemistry, 24 (1985) 6282.
20 Om P. Lamba, S. Lal, M.C. Yappert, M.F. Lou and D. Borchman, Biochim. Biophys. Acta, 1081 (1991) 181.
21 N. Delamere, C.A. Paterson, S. Cawood and D. Borchman, Am. J. Physiol., 260 (1991) C731.
22 R.G. Snyder, S.L. Hsu and S. Krimm, Spectrochim. Acta, Part A, 34 (1978) 395.
23 R.G. Snyder, H.L. Strauss and C.A. Elliger, J. Phys. Chem., 86 (1982) 5145.
24 M.R. Bunow and I.W. Levin, Biochim. Biophys. Acta, 487 (1977) 388.
25 L.J. Bellamy (Ed.), The Infrared Spectra of Complex Molecules, Chapman and Hall, London, 1975, pp. 233–245.
26 I. Pascher, Biochim. Biophys. Acta, 455 (1976) 433.
27 M.R. Bunow and I.W. Levin, Biophys. J., 32 (1980) 1007.
28 A.T. Tu, in R.J.H. Clark and R.E. Hester (Eds.), Advances in Infrared and Raman Spectroscopy, Vol. 13, Wiley, 1986, p. 47.
29 D.G. Cameron, H.L. Casal and H.H. Mantsch, Biochemistry, 19 (1980) 3665.
30 R.G. Snyder, J. Mol. Spectrosc., 7 (1961) 116.
31 J.R. Nielson and C.E. Hathaway, J. Mol. Spectrosc., 10 (1963) 366.
32 J.R. Arrondo, F.M. Goni and J.M. Macarulla, Biochim. Biophys. Acta, 794 (1984) 165.
33 D.G. Cameron and H.H. Mantsch, Biochim. Biophys. Res. Commun., 83 (1982) 886.
34 F. Bush, R.G. Adams and I.W. Levin, Biochemistry, 19 (1980) 4429.
35 Y. Barenholz, C. Schmidt and T.E. Thompson, Biochemistry, 16 (1977) 2649.
36 T.O. Henderson, T. Glonek and T.C. Meyers, Biochemistry, 13 (1974) 623.
37 F.M. Goni and J.R. Arrondo, Faraday Discuss. Chem. Soc., 86 (1986) 117.
38 R.G. Snyder, J. Chem. Phys., 47 (1967) 1316.
39 R.G. Snyder and J.H. Schachtschneider, Spectrochim. Acta, Part A, 19 (1963) 85.
40 B.P. Gaber and W.L. Peticolas, Biochim. Biophys. Acta, 465 (1977) 260.

41 H. Akutsu, Y. Suezaki, W. Yoshikawa and Y. Kyogoku, Biochim. Biophys. Acta, 854 (1986) 213.
42 E. Bicknell-Brown and K.G. Brown, Biochem. Biophys. Res. Commun., 94 (1980) 638.
43 K.G. Brown, E. Bicknell-Brown and M. Ladjadj, J. Phys. Chem., 91 (1987) 3436.
44 E. Bicknell-Brown, K.G. Brown and W.P. Person, J. Raman Spectrosc., 11 (1981) 356.
45 Om P. Lamba and H.D. Bist, J. Phys. Chem. Solids, 44 (1983) 445.
46 Om P. Lamba, H.D. Bist and D.P. Khandelwal, J. Mol. Struct., 101 (1983) 223.
47 Y. Baronholz, J. Suurkuusk, D. Mountcastle, T.E. Thompson and R.L. Biltonene, Biochemistry, 15 (1976) 2441.
48 W.I. Calhoun and G.G. Shipley, Biochim. Biophys. Acta, 555 (1979) 436.